A Stationary Phase Method for the Computation of the Far Field of Open Cassegrain Antennas

By W. H. IERLEY and H. ZUCKER

(Manuscript received October 17, 1969)

A method is presented for the computation of the far field radiation patterns of paraboloid reflector antennas by using a modified stationary phase approximation to eliminate one integration. This method is applicable to open cassegrain, offset paraboloid and horn reflector antennas. For symmetrical paraboloid antennas the modified approximation reduces to the exact expression obtained by direct integration.

The errors introduced by the stationary phase and modified stationary phase approximations are investigated. Specifically the far field of an open cassegrain with a 128 *wavelength aperture diameter is computed by the approximate method up to* 20 *degrees off-axis. The difference between these radiation patterns and those computed by double integration, is less than a few tenths of a* dB *up to* 1.0 *degree, and less than a few hundredths of a* dB *at larger angles off-axis.*

In order to estimate the computational advantage of this approximation, the number of points required for integration of an oscillatory function by Simpson's rule is also examined and it is determined that at least 6 *points per cycle are necessary to obtain* 4 *decimal accuracy. For fewer points the error is appreciable.*

I. INTRODUCTION

The computation of the far field radiation patterns of large reflector antennas is of importance in predicting the performance of satellite ground stations. For example, the antenna sidelobes contribute to the system noise temperature and may cause interference with other communication systems. The open cassegrain antenna[1] is a particularly suitable configuration for obtaining low sidelobe levels, since blocking by the subreflector and its supports are eliminated. A further advantage, resulting from this feature, is that the radiation pattern can be accurately predicted and it has been shown to be in good agreement with experimental results.[1]

The previous computations of the radiation patterns of open cassegrain antennas have been performed by precise computation of the appropriate diffraction integrals, generally requiring a double numerical integration. For large angles off-axis, such computations require considerable computation time. It is, however, for large angles that the integrals which are used for the computation of the far field radiation patterns are of a form which is suitable for approximation by the method of stationary phase. This method was initially applied to eliminate the azimuthal ϕ integration, but it was subsequently recognized that certain terms in the approximation are related to the asymptotic expansions of Bessel functions. The stationary phase approximation could therefore be modified, with the observed result that the far field radiation pattern can be computed with good accuracy also in the immediate vicinity of the main beam.

In the following sections we derive the stationary phase approximation and present a geometrical interpretation of the location of the stationary points. For the far field on axis, the ϕ integration is performed in closed form and it is shown that the antenna gain is the same for both perpendicular polarizations. Numerical computations are performed to estimate the error introduced by the stationary phase and modified methods. The extended range of applicability of the latter method is evident from the computations. The number of points per cycle needed to obtain an accurate value for an integral of an oscillatory function is also examined, and it is shown that for the functions considered at least 6 points/cycle are needed.

The far field radiation patterns of an open cassegrain with a 128 wavelength aperture diameter are computed with this method up to 20 degrees off-axis. In the vicinity of 20 degrees, the relative sidelobe levels are less than -65 dB or about 15 dB below isotropic.

1.1 *The Far Field*

The far electric field $\mathbf{E}_f$ of a paraboloid reflector antenna in an angular region about the axis, can be, based on the projected aperture field method, related to the reflected field at the aperture, $\mathbf{E}_r$, by the following expression:[2]

$$\mathbf{E}_f = \frac{j \exp(-jkR_a)}{\lambda R_a} \iint_A \mathbf{E}_r(x_p, y_p) \exp(jk\boldsymbol{\varrho}_p \cdot \mathbf{1}_{R_a})\, ds \tag{1}$$

where

λ = wavelength,
$k = 2\pi/\lambda$ (propagation constant),
R_a = the distance to the far field observation point,
$\boldsymbol{\varrho}_p$ is a vector in the aperture plane,
1_{R_a} is a unit vector which specifies the direction of the observation point,
A is the aperture area.

Specifically the direction of the observation point 1_{R_a} expressed in terms of the unit vectors of the aperture (x_p, y_p, z_p) coordinate system is:

$$1_{R_a} = 1_{x_p} \sin\theta_a \cos\phi_a + 1_{y_p} \sin\theta_a \sin\phi_a + 1_{z_p} \cos\theta_a \tag{2}$$

where θ_a and ϕ_a are the far field observation angles, and

$$\boldsymbol{\varrho}_p = 1_{x_p} x_p + 1_{y_p} y_p . \tag{3}$$

For an open cassegrain the incident fields at the main reflector can be more readily computed in a spherical coordinate system with the axis aligned with the horn subreflector axis as shown in Fig. 1. Therefore, the integrations in equation (1) are also performed in this coordinate system. The relations between aperture coordinates and the fields in the two coordinate systems were derived previously[1] and are

$$x_p = r[\cos\theta_0 \sin\theta \cos\phi + \sin\theta_0 \cos\theta], \tag{4}$$

$$y_p = r \sin\theta \sin\phi, \tag{5}$$

$$\begin{aligned} \frac{2f}{r}\mathbf{E}_r = {} & 1_{x_p}\{[\sin\theta_0 \sin\theta - \cos\phi(1 + \cos\theta\cos\theta_0)]E_\theta \\ & + \sin\phi(\cos\theta + \cos\theta_0)E_\phi\} \\ & - 1_{y_p}\{\sin\phi(\cos\theta_0 + \cos\theta)E_\theta \\ & - [\sin\theta\sin\theta_0 - \cos\phi(1 + \cos\theta\cos\theta_0)]E_\phi\}, \end{aligned} \tag{6}$$

where E_θ and E_ϕ are the θ and ϕ components of the incident electric field, f is the focal length of the paraboloid and r is the equation of the paraboloid surface in the θ, ϕ coordinate system

$$r = \frac{2f}{1 + \cos\theta_0 \cos\theta - \sin\theta \sin\theta_0 \cos\phi} \tag{7}$$

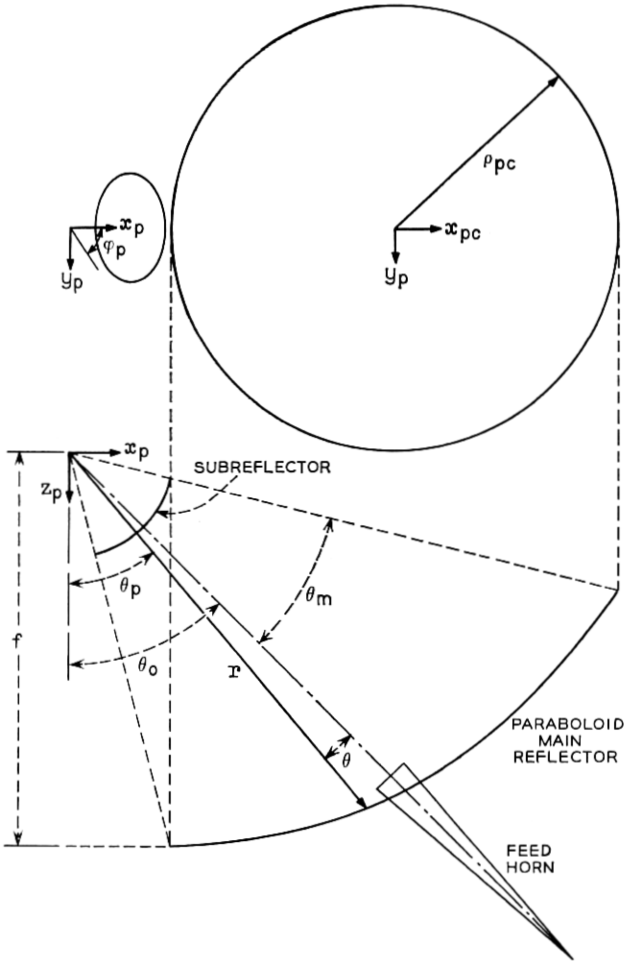

Fig. 1 — Open cassegrain antenna.

θ_0 is the offset angle. The surface element

$$ds = r^2 \sin \theta \, d\theta \, d\phi. \tag{8}$$

Heretofore the above integral has been evaluated by double integration using Simpson's rule. Although rather accurate results can be obtained in this fashion, computation time for a given angle, θ_a increases roughly proportional to $(\sin \theta_a)^2$ (see Appendix C). As a result, except for the mainlobe and first few sidelobes of the far field, this approach becomes extremely time consuming. To reduce the computation time for large values of the off-axis angle θ_a , the stationary phase approximation to the ϕ integration is investigated.

1.2 *The Method of Stationary Phase*

Consider an integral of the form

$$I(k \sin \theta_a) = \int_a^b g(\phi) \exp \{j(k \sin \theta_a)\psi(\phi)\} \, d\phi \tag{9}$$

where $(k \sin \theta_a)$ is large, $\psi(\phi)$ is a real function and $g(\phi)$ is a slowly varying function. The method of stationary phase[3] approximates the above integral to $O(1/k \sin \theta_a)$ by considering only contributions in the vicinity of the stationary points ϕ_i where $\psi'(\phi_i) = 0$.

Under these conditions

$$I(k \sin \theta_a) \approx \sum_i g(\phi_i)\left(\frac{2j\pi}{k \sin \theta_a \psi''(\phi_i)}\right)^{\frac{1}{2}} \exp \{jk \sin \theta_a \psi(\phi_i)\}. \tag{10}$$

This method has been applied to the ϕ integration in the expression for the far field (1).

From equations (1), (2) and (3) $\psi(\phi)$ can be written as

$$\psi(\phi) = [1_{x_p} \cos \phi_a + 1_{y_p} \sin \phi_a] \cdot \boldsymbol{\varrho}_p \, . \tag{11}$$

For specified observation angles θ_a and ϕ_a , equation (11) can be considered as the projection of the vector $\boldsymbol{\varrho}_p$ in the direction of the unit vector $1_{\rho_a} = 1_{x_p} \cos \phi_a + 1_{y_p} \sin \phi_a$. For the problem under consideration $\boldsymbol{\varrho}_p$ is a function of θ and ϕ. It has been shown previously[1] that for constant θ, the vector $\boldsymbol{\varrho}_p$ describes a circle as ϕ varies from 0 to 2π. The equation of the circle is

$$\left(x_p - \frac{2f \sin \theta_0}{\cos \theta_0 + \cos \theta}\right)^2 + y_p^2 = \left(\frac{2f \sin \theta}{\cos \theta + \cos \theta_0}\right)^2. \tag{12}$$

A family of such circles for an offset angle θ_0 of 47.5° is shown in Fig. 2.

Therefore the condition $\psi'(\phi) = 0$ corresponds to determining the extreme values of the projections of the vector $\boldsymbol{\varrho}_p$ in the direction of the unit vector 1_{ρ_a} . It is evident from Fig. 2 that as $\boldsymbol{\varrho}_p$ describes a constant θ circle two extreme values for the projections exist, namely at those two points on the circle such that tangents to the circle passing through the points intersect normally a line in the direction of the unit vector 1_{ρ_a} . Furthermore the difference between the two extreme projections is the circle diameter.

The expressions for the stationary points and the other values which enter in the evaluation of the ϕ integration are derived in Appendix A.

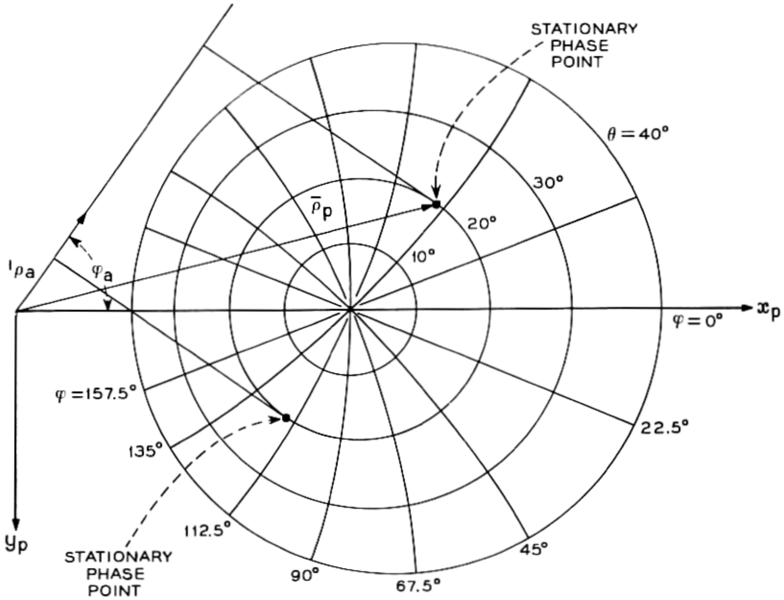

Fig. 2 — Projection circles of the paraboloid reflector for $\theta_0 = 47.5°$.

1.3 *Approximate Values*

In order to approximate the ϕ integration in equation (1), namely

$$\mathbf{E} = \int_0^{2\pi} r^2 \mathbf{E}_r \exp \{jk \sin \theta_a (x_p \cos \phi_a + y_p \sin \phi_a)\} \, d\phi \qquad (13)$$

by the stationary phase method, the reflected field $\mathbf{E}_r$ has to be determined at the stationary points. This field has an explicit ϕ dependence for a TE_{11} mode or combined $TE_{11} - TM_{11}$ excitation. For these modes it has been shown[1] that for x and y polarization the field components E_θ and E_ϕ are

$$x \text{ polarization} \begin{cases} E_\theta = E(\pi/2) \cos \phi & (14) \\ E_\phi = -E(0) \sin \phi & (15) \end{cases}$$

$$y \text{ polarization} \begin{cases} E_\theta = E(\pi/2) \sin \phi & (16) \\ E_\phi = E(0) \cos \phi & (17) \end{cases}$$

where $E(\pi/2)$ and $E(0)$ denote the θ dependence of the fields when the feed horn is excited for y polarization in the planes $\phi = \pi/2$ and $\phi = 0$, respectively.

As shown in Appendix A, it is sufficient to evaluate the fields at the stationary points for one polarization only. For the other polarization the fields are then readily obtained. Therefore only y polarization will be considered. Furthermore it will be assumed that the radiated field from the subreflector has been computed at a constant radius from the focal point of the hyperboloid subreflector.

By assuming a $1/r$ dependence for subreflector fields, the relation between the fields is

$$\mathbf{E}_r(\theta, \phi) = \frac{2f}{1 + \cos\theta_0} \frac{\mathbf{E}_c(\theta, \phi)}{r} \tag{18}$$

where $\mathbf{E}_c$ is the field at the distance $2f/(1 + \cos\theta_0)$ and r is the equation of the paraboloid (7). The spherical phase dependence of the field in equation (18) is suppressed.

With the approximation (18) and the stationary phase approximation to the ϕ integration, the far field using equation (1) is obtained from the integral (see Appendix A)

$$(\mathbf{E}_{fy}) = j \frac{\exp(-jkR_a)}{\lambda R_a} \int_0^{\theta_m} (\mathbf{E}_y) \sin\theta \, d\theta \tag{19}$$

where the subscript y designates that the far field is for y polarization, and θ_m is the illumination angle. The y and x (cross polarization) components of $(\mathbf{E}_y)$ namely $(E_y)_y$ and $(E_y)_x$ are given by

$$(E_y)_y = \frac{-\pi(2f)^2 e^{i\beta}}{c(a^2 - b^2\cos^2\phi_a)(1 + \cos\theta_0)} \left[\frac{2}{\pi\left(\alpha + \frac{\pi}{4}\right)}\right]^{\frac{1}{2}}$$

$$\cdot [c(e^{i\alpha} + e^{-i\alpha})\{a \sin^2\phi_a \, E_c(\pi/2) + c\cos^2\phi_a \, E_c(0)\}$$

$$- b\sin^2\phi_a \cos\phi_a (e^{i\alpha} - e^{-i\alpha})\{cE_c(\pi/2) - aE_c(0)\}] \tag{20}$$

and the cross polarized component $(E_y)_x$ is

$$(E_y)_x = \frac{\pi(2f)^2 e^{i\beta}\sin\phi_a}{c(a^2 - b^2\cos^2\phi_a)(1 + \cos\theta_0)} \left[\frac{2}{\pi\left(\alpha + \frac{\pi}{4}\right)}\right]^{\frac{1}{2}}$$

$$\cdot [b(e^{i\alpha} - e^{-i\alpha})\{a\sin^2\phi_a \, E_c(0) + c\cos^2\phi_a \, E_c(\pi/2)\}$$

$$+ c\cos\phi_a(e^{i\alpha} + e^{-i\alpha})\{cE_c(0) - aE_c(\pi/2)\}] \tag{21}$$

where

$$a = 1 + \cos\theta\cos\theta_0, \tag{22a}$$

$$b = \sin\theta \sin\theta_0, \tag{22b}$$

$$c = \cos\theta + \cos\theta_0. \tag{22c}$$

$$\alpha = \frac{2kf \sin\theta_a \sin\theta}{\cos\theta + \cos\theta_0} - \pi/4, \tag{23}$$

$$\beta = 2kf \sin\theta_a \cos\phi_a \left[\frac{\sin\theta_0}{\cos\theta + \cos\theta_0} - \frac{\sin\theta_m}{\cos\theta_0 + \cos\theta_m}\right]. \tag{24}$$

The second term in equation (24) reduces the phase by a constant.

The expansions (20) and (21) are valid for ($k \sin\theta_a$) very large. It should be noted that (20) and (21) display singularities at $\alpha = -\pi/4$, that is, at $\theta_a = 0$, or $\theta = 0$. However, upon examination it can be seen that (20) and (21) contain the first terms of the asymptotic expansions for Bessel functions, that is,

$$\begin{aligned} J_n(x) &\sim \left(\frac{2}{\pi x}\right)^{\frac{1}{2}} \cos\left(x - \frac{n\pi}{2} - \frac{\pi}{4}\right) \\ &\sim \frac{1}{2}(j)^n\left(\frac{2}{\pi x}\right)^{\frac{1}{2}}\left\{(-1)^n \exp\left[j\left(x - \frac{\pi}{4}\right)\right] + \exp\left[-j\left(x - \frac{\pi}{4}\right)\right]\right\}. \end{aligned} \tag{25}$$

By identifying and replacing the asymptotic terms by the actual Bessel functions, the singularities are removed and it might be expected that the approximation for small θ and θ_a would improve and furthermore for large values of θ and θ_a the approximations would be equivalent. There is however, no unique method to introduce such a replacement. The method chosen was dictated by the requirement that for the symmetric case $\theta_0 = 0$, the expressions reduce to the exact expressions previously determined.[4] This necessitates associating a Bessel function of order n, $J_n(x)$ with terms $\cos n\phi_a$ or $\sin n\phi_a$.

On this basis the approximations to the ϕ integration are:

$$\begin{aligned} (E_y)_y = {} & \frac{-\pi(2f)^2 e^{j\beta}}{c(a^2 - b^2\cos^2\phi_a)(1 + \cos\theta_0)} \\ & \cdot [c(J_0(x)\{aE_c(\pi/2) + cE_c(0)\} + J_2(x)\cos 2\phi_a\{aE_c(\pi/2) - cE_c(0)\}) \\ & - j/2b\{cE_c(\pi/2) - aE_c(0)\}\{J_1(x)\cos\phi_a + J_3(x)\cos 3\phi_a\}] \end{aligned} \tag{26}$$

and the cross polarized component

$$\begin{aligned} (E_y)_x = {} & \frac{\pi(2f)^2 e^{j\beta}}{c(a^2 - b^2\cos^2\phi_a)(1 + \cos\theta_0)} \\ & \cdot [jb\{3aE_c(0) + cE_c(\pi/2)\}J_1(x)\sin\phi_a \\ & + 2c\{aE_c(\pi/2) - cE_c(0)\}J_2(x)\sin 2\phi_a \\ & + jb\{aE_c(0) - cE_c(\pi/2)\}J_3(x)\sin 3\phi_a] \end{aligned} \tag{27}$$

where

$$x = \frac{4\pi f}{\lambda}\left(\frac{\sin\theta_a \sin\theta}{\cos\theta + \cos\theta_0}\right). \tag{28}$$

It is noted the $(E_y)_y$ is symmetrical with respect to ϕ_a since by interchanging ϕ_a by $-\phi_a$ the expression remains the same. This would be expected since the plane $\phi = 0$ is a plane of antenna symmetry. It is also evident from equation (27) that the cross polarized component is zero in the plane of symmetry and is antisymmetrical with respect to ϕ_a.

The above expressions reduce to those obtained by the method of stationary phase for large values of x. As shown subsequently by numerical integration the latter approximations extend considerably the range of θ and θ_a beyond which the stationary phase approximations are applicable.

For x polarization as outlined in Appendix A the expressions are similar. In particular $(E_x)_x$ is of the same form as $(E_y)_y$ with $E_c(o)$ and $E_c(\pi/2)$ interchanged. The cross polarized component $(E_x)_y$ is of the same form as $-(E_y)_x$ with $E_c(o)$ and $E_c(\pi/2)$ interchanged.

The expressions (26) and (27) are of course approximate. This is evident by considering the special case $\theta_a = 0$, where the values for the fields must be the same independent of ϕ_a. For this special case the ϕ integration is performed in closed form in Appendix B.

For the antenna shown in Fig. 1, with $\theta_0 = 55°$ and $\theta_m = 34.0°$, by assuming the radiation fields of the subreflector at a constant distance are the same in the E and H planes, it is shown that the differences between the exact and the approximate values at $\theta_a = 0$ are 0.049 in the E-plane and -0.053 in the H-plane, both in comparison to one. The subsequent numerical computations indicate that these are the largest errors introduced by the approximation.

1.4 *Numerical Results*

In order to determine the validity of the above approximations, computations of the far field radiation patterns for the open cassegrain antenna have been performed using the subreflector radiation pattern $\mathbf{E}_c$ shown in Fig. 3.

The integration with respect to ϕ, as indicated in equation (13), has been performed, employing Simpsons rule, as a function of θ in the E and H planes, and for observation angles $\theta_a = 0$, 2.5, 5°, 10° and 20°. Estimates for the number of points required for the ϕ integration and the computation time are presented in Appendix C.

The normalized amplitudes obtained from the integration are shown in the upper portions of Figs. 4–8. The normalization was based on the

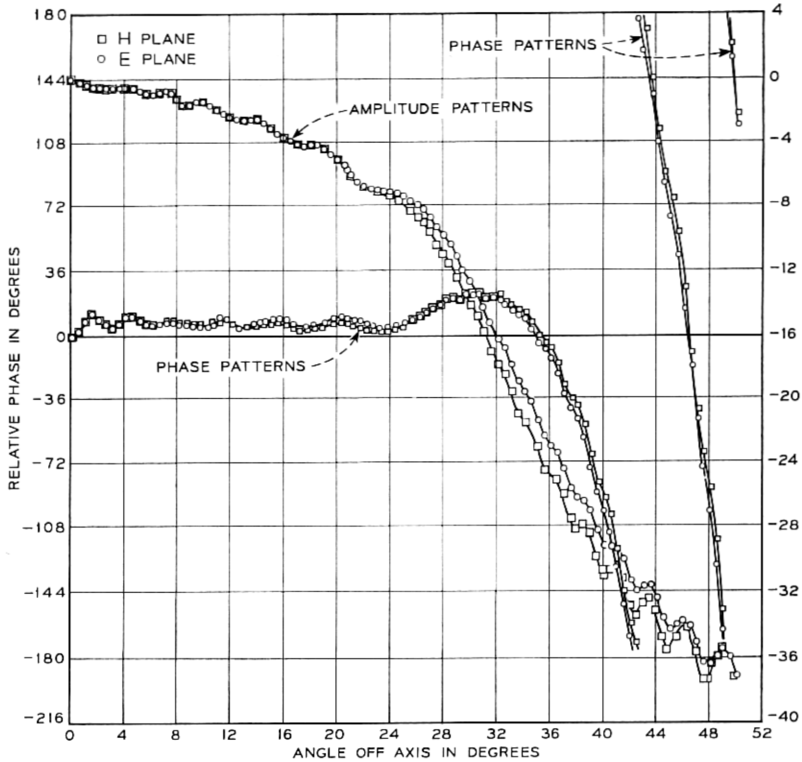

Fig. 3 — Amplitude and phase of subreflector radiation pattern.

stationary phase approximation (20) which shows that in the planes $\phi_a = 0$ or $\pi/2$ the integral (13) is proportional to $E_c(o)$ or $E_c(\pi/2)$ respectively. The normalized values for the integrals E_N shown are

$$E_N = \frac{(E_y)_y/E_c}{[(E_y)_y/E_c]_0} \tag{29}$$

where the subscript zero indicates the value at $\theta = 0$.

Immediately beneath E_N in Figs. 5–8 is shown a plot of the absolute value of the difference between the normalized values obtained by integration and the stationary phase approximation given by equation (20). The third plot in each figure show the corresponding difference using the modified stationary phase approximation (26). As predicted by the method of stationary phase and as shown in Figs. 5–8, the approximations improve as $k \sin \theta_a$ increases. However, where as for small values of θ the stationary phase approximation (20) introduces significant error, the modified approximation (26) becomes increasingly accurate. It should also be noted that with both approximations relative maximum differences occur near zeros, therefore resulting in less significance in the second integration.

Figures 9 and 10 show the amplitudes of the far field radiation as computed by single integration and the modified stationary phase approximation (26). Shown for y polarization are the far field in the plane of antenna symmetry $\phi_a = 0$ and π, and the fields in the plane of asymmetry $\phi_a = \pi/2$ up to 20° off axis. Figure 11 shows the difference in the plane $\phi_a = 0$ between the far field pattern computed by the approximate method and the same pattern computed using double integration. Excluding the vicinity of relative minima, errors were less than 0.2 dB up to off-axis angles of 1°, and on the order of a few hundredths of a dB for larger angles. It should be noted that on axis the difference is zero, since the exact expression for the ϕ integration as given in Appendix B is incorporated in the single integration program.

II. CONCLUSIONS

A method has been developed for the numerical computation of the far field radiation patterns of open cassegrain antennas and related

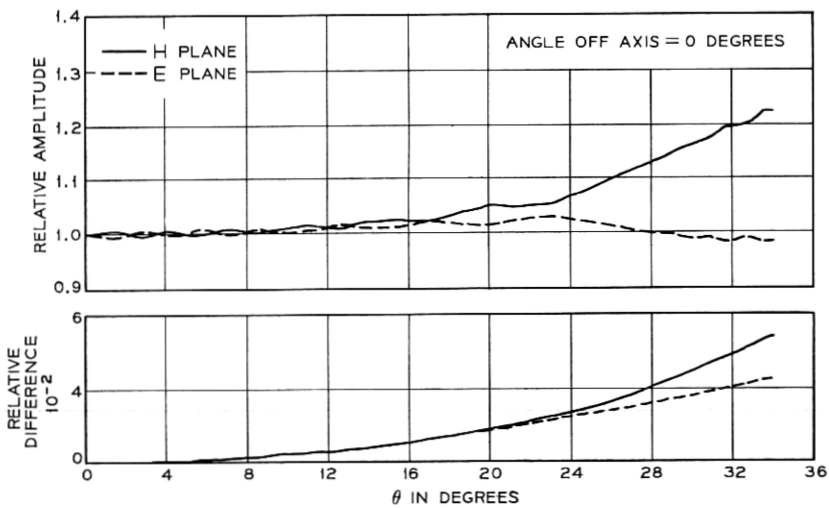

Fig. 4 — Error introduced by modified approximation [equation (26)] on axis.

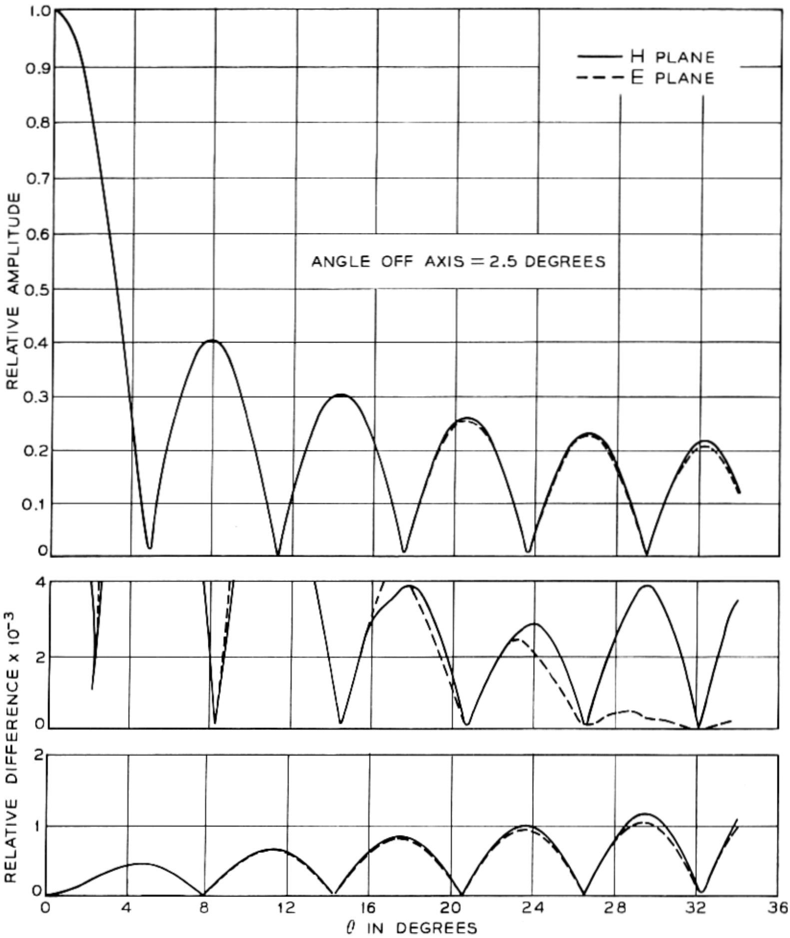

Fig. 5 — Error introduced by stationary phase approximation [equation (20)] and modified approximation [equation (26)].

antenna configurations using a single numerical integration, which reduces considerably the computation time. The method is based on the stationary phase approximation but modified such that for symmetrical paraboloid antennas the approximation reduces to the exact expression which is obtained by direct integration. The errors introduced by stationary phase and modified approximations are examined. It is shown by numerical computations that the error in the far field radiation pattern introduced by the modified stationary phase approximation at angles beyond the main beam is on the order of a few hundreths of a dB.

The number of points needed for numerical integration of oscillatory functions by Simpson's rule is also examined by using specific oscillatory functions. It was determined that at least 6 points per cycle are necessary to obtain four decimal-point accuracy.

The radiation patterns of an open cassegrain antenna with a 128 wavelength aperture diameter are computed up to 20° off axis. In this

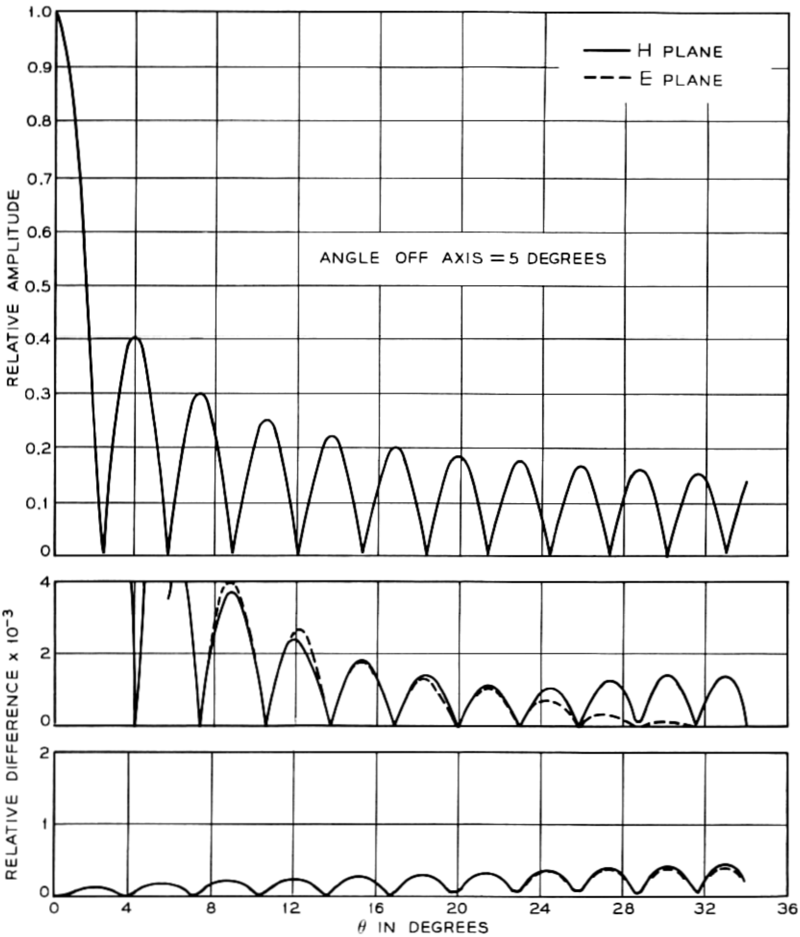

Fig. 6 — Error introduced by stationary phase approximation [equation (20)] and modified approximation [equation (26)]

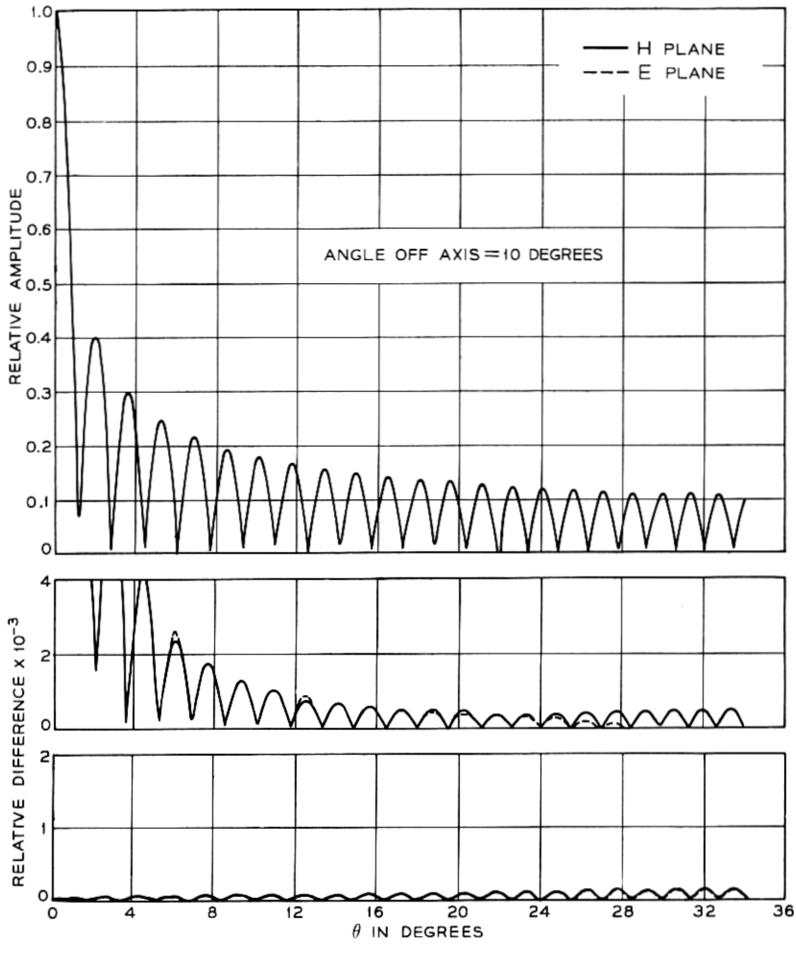

Fig. 7 — Error introduced by stationary phase approximation [equation (20)] and modified approximation [equation (26)].

region the sidelobe levels are −65 dB or −15 dB below the isotropic levels.

Although the stationary phase method has been applied here to the computation of the far field based on the projected aperture field method, the same approach may be used for the computations based on the current distribution method. In particular in the plane of antenna symmetry, the locations of the stationary phase stationary points are the same and therefore the presented approximations are readily extended to this plane.

APPENDIX A

Derivation of the Stationary Phase Approximation

Consider the ϕ integration of equation (1)

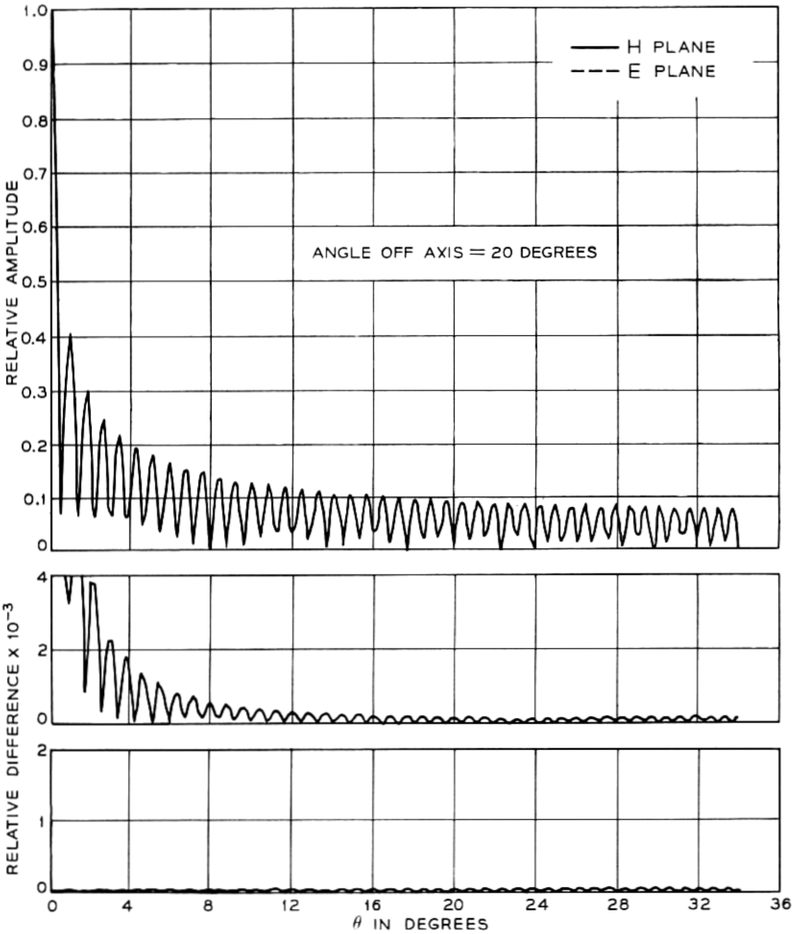

Fig. 8 — Error introduced by stationary phase approximation [equation (20)] and modified approximation [equation (26)].

$$\mathbf{E}(k,\ \theta) = \int_0^{2\pi} \mathbf{E}_r(\theta,\ \phi) \exp\ [jk \sin\ \theta_a(x_p\ \cos \phi_a\ +\ y_p \sin \phi_a)]r^2\ d\phi \qquad (30)$$

with x_p , y_p , $\mathbf{E}_r$ and r given by equations (4) through (7). The stationary points are determined by

$$\frac{\partial x_p}{\partial \phi} \cos \phi_a + \frac{\partial y_p}{\partial \phi} \sin \phi_a = \frac{d\psi}{d\phi} = 0. \qquad (31)$$

This leads to the relation

$$[(1 + \cos\theta \cos\theta_0) \cos\phi - \sin\theta \sin\theta_0] \sin\phi_a - \sin\phi[\cos\theta + \cos\theta_0] \cos\phi_a = 0. \qquad (32)$$

Equation (32) is a quadratic equation in cos ϕ. Solving this equation

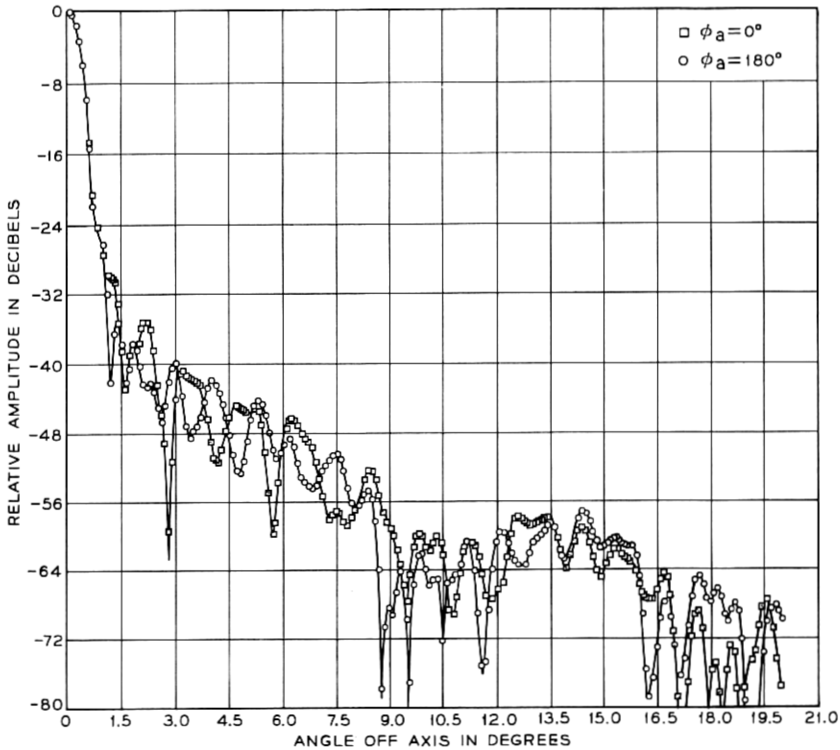

Fig. 9 — Far field radiation pattern in the plane of symmetry.

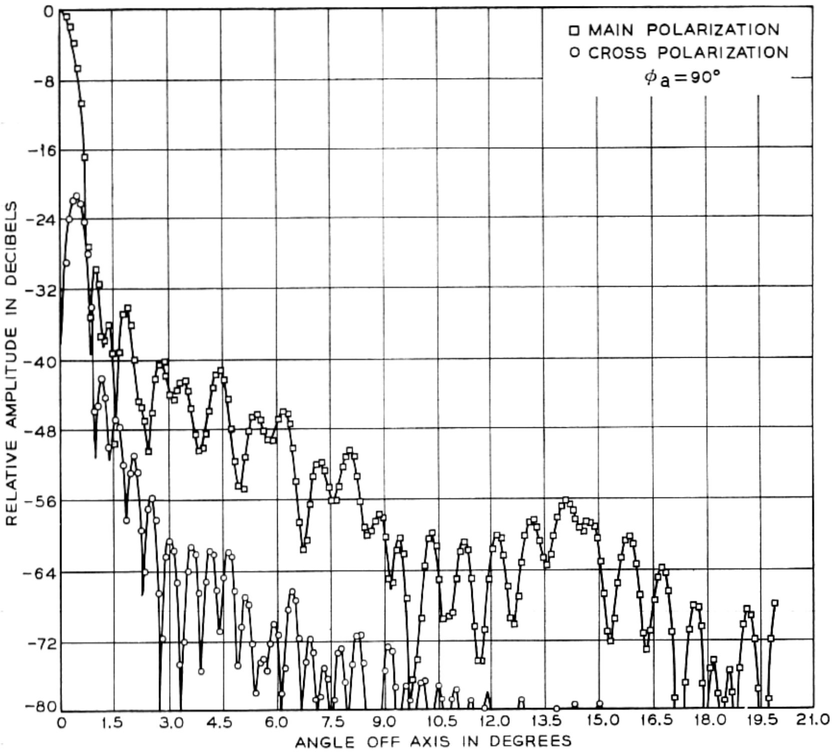

Fig. 10 — Far field radiation pattern in the plane of asymmetry.

yields the following values for the stationary points

$$\cos \phi_{1,2} = \frac{\sin \theta \sin \theta_0 \pm \cos \phi_a(1 + \cos \theta \cos \theta_0)}{1 + \cos \theta \cos \theta_0 \pm \cos \phi_a \sin \theta \sin \theta_0} \tag{33}$$

and from (32)

$$\sin \phi_{1,2} = \pm \frac{\sin \phi_a(\cos \theta + \cos \theta_0)}{1 + \cos \theta \cos \theta_0 \pm \cos \phi_a \sin \theta \sin \theta_0}. \tag{34}$$

Evaluating the phase factor ψ gives

$$\psi(\phi_1) = 2f \frac{(\sin \theta + \cos \phi_a \sin \theta_0)}{\cos \theta + \cos \theta_0}; \tag{35}$$

$$\psi(\phi_2) = -2f \frac{(\sin \theta - \cos \phi_a \sin \theta_0)}{\cos \theta + \cos \theta_0}. \tag{36}$$

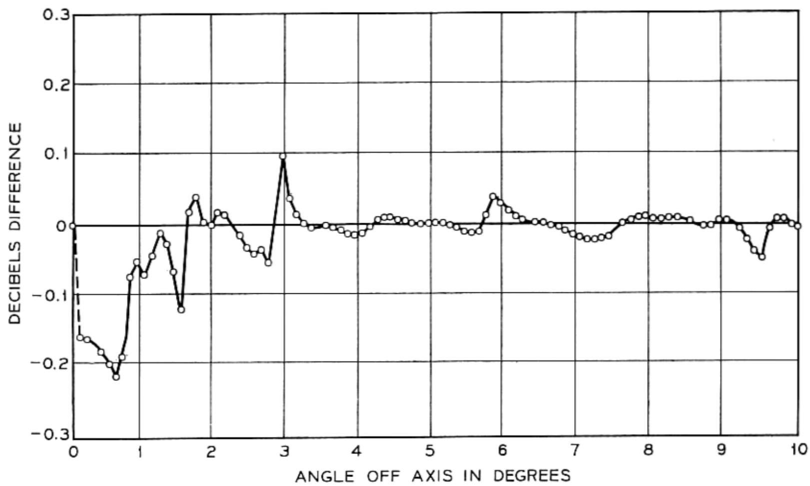

Fig. 11 — Difference in far field pattern as computed by double integration and approximate method (in the plane $\phi_a = 0$).

Note that

$$\psi(\phi_1) - \psi(\phi_2) = 2\left[\frac{2f \sin \theta}{\cos \theta + \cos \theta_0}\right] \tag{37}$$

which is the diameter of the circle given by equation (12). That is the stationary points are antipodes on the projection of the plane of the intersection of the paraboloid surface with the cone θ = constant.

Evaluation of the second derivative leads to

$$\left.\frac{d^2\psi}{d\phi^2}\right|_{1,2} = \mp 2f \sin \theta \frac{[1 + \cos \theta \cos \theta_0 \pm \cos \phi_a \sin \theta \sin \theta_0]^2}{[\cos \theta + \cos \theta_0]^3}. \tag{38}$$

Evaluation of r gives

$$r_{1,2} = 2f \frac{[1 + \cos \theta \cos \theta_0 \pm \sin \theta \sin \theta_0 \cos \phi_a]}{[\cos \theta + \cos \theta_0]^2}. \tag{39}$$

It remains to evaluate $\mathbf{E}_r$ at the stationary points. From equation (18)

$$\mathbf{E}_r = \frac{\mathbf{E}_c}{r} \frac{2f}{(1 + \cos \theta_0)}. \tag{40}$$

From equations (6) and (31)

$$(\mathbf{E}_r)_{1,2} = -\frac{\sin \phi_{1,2}}{\sin \phi_a} \frac{(\cos \theta + \cos \theta_0)}{1 + \cos \theta_0} [1_{xp}(E_{c\theta} \cos \phi_a - E_{c\phi} \sin \phi_a) + 1_{yp}(E_{c\theta} \sin \phi_a + E_{c\phi} \cos \phi_a)]. \tag{41}$$

Substituting the values for x and y polarization in equations (14) through (17) it is evident that the expressions are similar. Therefore the x component for x polarization can be obtained from the y component for y polarization by interchanging $E_c(o)$ with $E(\pi/2)$. Similarly the y component for x polarization can be obtained from the x component for y polarization also by interchanging $E_c(o)$ with $E(\pi/2)$ and changing the sign in front of the resulting expression.

Substituting the appropriate expressions for y polarization into the stationary phase approximation leads to equations (20) and (21).

APPENDIX B

The ϕ Integration on Axis ($\theta_a = 0$)

From equations (6), and (13) for $\theta_a = 0$, the integral for the y component of y polarization with respect to ϕ can be written

$$(E_y)_y = -\frac{(2f)^2}{(1 + \cos\theta_0)} \cdot \int_0^{2\pi} \left\{ \frac{[E_c(\pi/2)c - aE_c(0)]\sin^2\phi}{[a - b\cos\phi]^2} + \frac{E_c(0)}{a - b\cos\phi} \right\} d\phi \tag{42}$$

where a, b, and c are defined by equations (22a), (22b), and (22c). Integrating the first term by parts, reduces the evaluation of equation (42) to a tabulated integral,[5] that is,

$$\int_0^{2\pi} \frac{d\phi}{a - b\cos\phi} = \frac{2\pi}{(a^2 - b^2)^{\frac{1}{2}}} \tag{43}$$

hence

$$(E_{ry})_y = -2(2f)^2 \frac{[E_c(\pi/2) + E_c(0)]}{(1 + \cos\theta_0)^2(1 + \cos\theta)}. \tag{44}$$

The integration for x polarization $(E_{rx})_x$ gives the same result. As a consequence the on-axis gain for an open cassegrain antenna is the same for x and y polarization if the excitation is the same. Based on the approximation (26)

$$(E_y)_y = -\frac{(2f)^2[E_c(\pi/2)(1 + \cos\theta\cos\theta_0) + E_c(0)(\cos\theta + \cos\theta_0)]}{(1 + \cos\theta_0)[(1 + \cos\theta\cos\theta_0)^2 - (\sin\theta\sin\theta_0\cos\phi_a)^2]}. \tag{45}$$

To estimate the relative error it is assumed that $E_c(o) = E_c(\pi/2)$. This gives in the plane $\phi_a = 0$ or π

$$(\Delta E_y)_y = 1 - \left[\frac{(1 + \cos\theta)(1 + \cos\theta_0)}{2[\cos\theta + \cos\theta_0]}\right]^2.$$

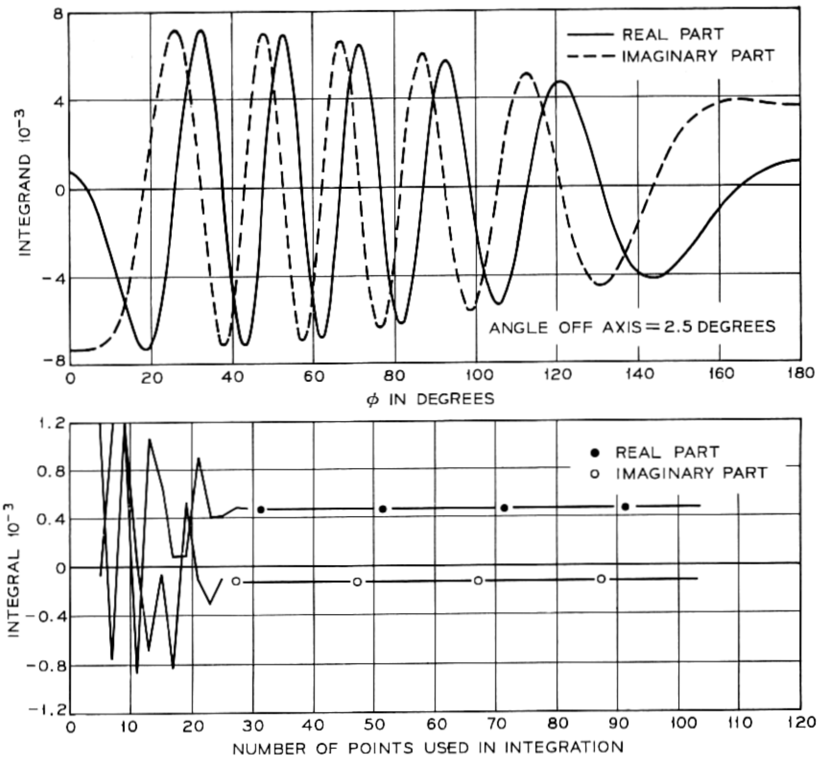

Fig. 12 — Numerical integration of oscillatory function.

Similarly in the plane $\phi_a = \pi/2$

$$(\Delta E_y)_y = 1 - \left[\frac{(1 + \cos\theta)(1 + \cos\theta_0)}{2(1 + \cos\theta\cos\theta_0)}\right]^2. \tag{46}$$

Equations (48) and (49) can be combined yielding

$$(\Delta E_y)_y = 1 - \frac{1}{[1 \pm (\tan\theta/2 \tan\theta_0/2)^2]^2} \tag{47}$$

where the minus sign corresponds to $\phi = 0$ or π and the plus sign is for $\phi_a = \pi/2$.

APPENDIX C

Computation Time Estimates

The attempt to find a suitable approximation to be used for the evaluation of far field radiation patterns was motivated, in fact necessitated, by the excessive computation time required for a double integration procedure.

Both the ϕ integral [equation (13)] and the θ integral [equation (19)] have oscillatory integrands, with the ϕ integrand, for the maximum value of θ, having approximately double the number of oscillations as the θ integrand. The maximum number of full cycles in the θ integrand is equal approximately to

$$\frac{D}{2\lambda} \sin \theta_a$$

where D is the antenna aperture diameter.

Figures 12 through 15 show the ϕ integrand for $\theta = 34°$, and for various values of observation angle θ_a . Below these figures is shown

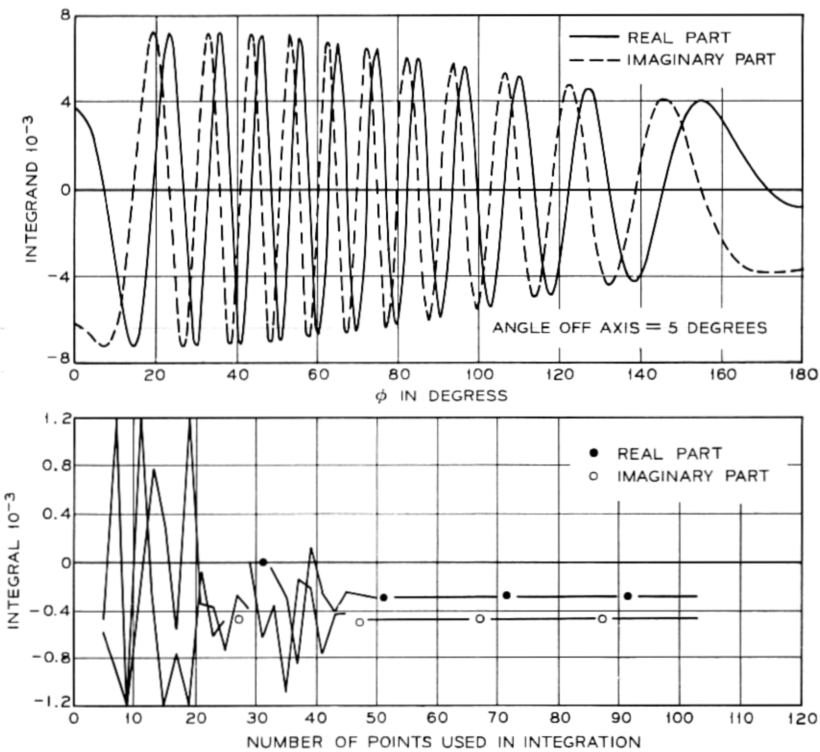

Fig. 13 — Numerical integration of oscillatory function.

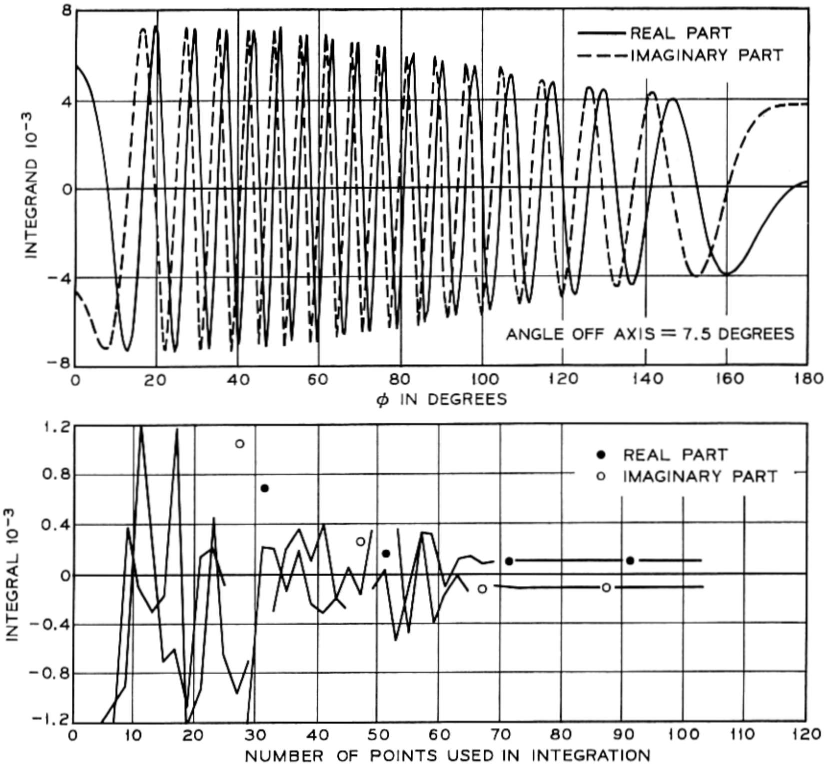

Fig. 14 — Numerical integration of oscillatory function.

the result of the ϕ integration using Simpson's rule with increasing number of points. We have found by numerical integration that for the integrands discussed above, a minimum number of 6 points per cycle is necessary to provide reasonable accuracy.

For a discussion of numerical integration of oscillatory integrands the reader is referred to Ref. 6.

An estimate for the processor time required to calculate both components of the far field pattern in both the E and H planes (4 patterns) out to an observation angle of θ_a degrees by the method of double integration is given by:

$$k_2 \frac{\theta_a}{\Delta\theta_a} N^2 \frac{\theta_a^2}{3}$$

where

k_2 is the fundamental program loop execution time (1.13×10^{-4} min., on the G. E. 635).

N is the number of integrand evaluations per cycle required by the integration procedure.

$\Delta\theta_a$ is the observation angular increment at which results are to be calculated.

An estimate for the same calculation by the approximate method derived herein is:

$$k_1 \frac{\theta_a}{\Delta\theta_a} N \frac{\theta_a}{2}$$

where

$$k_1 = 0.75 \times 10^{-3} \text{ min.}$$

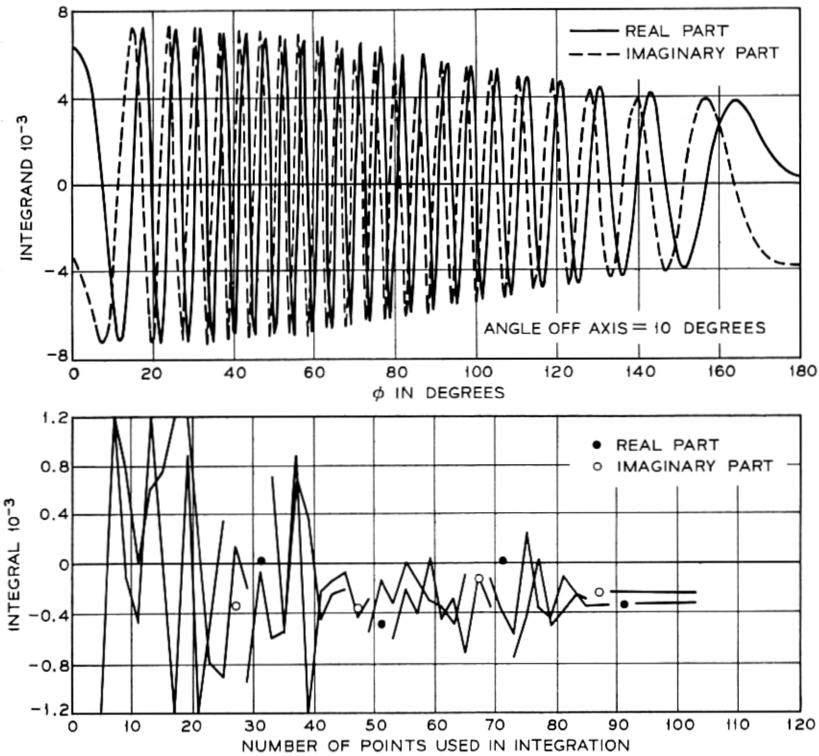

Fig. 15 — Numerical integration of oscillatory function.

TABLE I—EXECUTION TIMES

θ_a	5°	10°	20°
Double Int.	4.7 min.	38 min.	300 min.
Appr. Method	0.9 min.	3.7 min.	15 min.

Table I shows comparable execution times for various observation angle extremes, assuming $\Delta\theta_a = 0.1°$, $N = 10$.

REFERENCES

1. Cook, J. S., Elam, E. M., and Zucker, H., "The Open Cassegrain Antenna," B.S.T.J., *44*, No. 7 (September 1965), pp. 1255–1300.
2. Silver, S., *Microwave Antenna Theory and Design,* New York: McGraw-Hill, 1949.
3. Erdelyi, A., *Asymptotic Expansions,* New York: Dover Publ., 1950, pp. 51–57.
4. Zucker, H., and Ierley, W. H., "Computer Aided Analysis of Cassegrain Antennas," B.S.T.J., *47*, No. 6 (July-August 1968), pp. 897–932.
5. Dwight, H. B., *Tables of Integrals and Other Matehmatical Data,* New York: The MacMillan Company, 1957, p. 199.
6. Allen, C. C., "Numerical Integration Methods for Antenna Pattern Calculations," IRE Transactions on Antennas and Propagation, Special Supplement, Symposium on Electromagnetic Theory, December 1959, pp. 387–401.